2D Ising Model

PHYS 547
Soft and Active Matter Physics
https://github.com/Omerdkmc/PHYS-547

Ömer Fatih Dokumacı
Alp Ünlü
Tuna Tülümen

1 Introduction

Originally proposed to describe ferromagnetism by Wilhelm Lenz in 1920 and studied by Ernst Ising, who famously solved the 1D case in 1925, the Ising model is a central model in statistical physics. It is a system of spins, usually in 1D or 2D lattice, with a spin at each lattice site i. And each spin in this lattice can take a discrete spin value $\sigma_i = \pm 1$. In this system, in the case of ferromagnetic coupling, alignment of two neighboring spins ($\sigma_i \sigma_j = +1$) corresponds to the lower energy state, and on the contrary, it is a high energy state if the spins are anti-parallel ($\sigma_i \sigma_j = -1$). Despite its simplicity, the 2D Ising model exhibits a phase transition: at high temperature T, thermal fluctuations disorder the spins and the equilibrium magnetization vanishes in the thermodynamic limit, while below a critical temperature T_c the system spontaneously orders into a magnetized phase with large domains of aligned spins.

It is possible to study equilibrium properties or domain coarsening of the system. The study of the model is typically done by Monte Carlo sampling methods, which generate spin configurations distributed according to the Boltzmann distribution. Metropolis algorithm is one of the simpler methods in this regard and thus, is employed in this work to simulate the 2D Ising model. Here, we find the critical temperature T_c from equilibrium observables and characterize domain coarsening by utilizing a Floodfill cluster finding algorithm.

This report is structured as follows: first, we present the theoretical background of the model, then describe the numerical methods used, and finally present and discuss the results.

2 Theory

2.1 2D Ising Model

2D Ising model is defined on a two dimensional lattice with a spin at each site i and the Hamiltonian of the system is:

$$H = -J \sum_{<ij>} \sigma_i \sigma_j - h \sum_i \sigma_i \tag{1}$$

where $J > 0$ is the interaction coefficient and $< ij >$ represents the sum over first neighbors in the system. The first term is the exchange integral, which represents the tendency of first neighbor spins to align with each other. The second term describes the alignment interaction in the presence of a magnetic field.

To study the system at thermal equilibrium at some temperature T we can use the canonical ensemble. In such an ensemble the probability of a spin configuration $\{\sigma\}$ is given by the Boltzmann distribution

$$P(\{\sigma\}) = \frac{1}{Z} e^{-\beta H(\{\sigma\})}, \qquad \beta = \frac{1}{k_B T}, \tag{2}$$

where the partition function $Z = \sum_{\{\sigma\}} e^{-\beta H(\{\sigma\})}$ is used to normalize the distribution. Thermal expectation values of thermodynamical observables $\mathcal{O}$ can be computed as

$$\langle \mathcal{O} \rangle = \sum_{\{\sigma\}} \mathcal{O}(\{\sigma\})\, P(\{\sigma\}). \tag{3}$$

2.2 Symmetry Breaking and Order Parameter

In the absence of external field, the second term in Equation 1 can be omitted:

$$H = -J \sum_{<ij>} \sigma_i \sigma_j \tag{4}$$

In this case, under a global spin-flip transformation $\mathcal{P}$, the Hamiltonian is invariant for any spin configuration $\{\sigma\}$.

$$\mathcal{P} : \sigma_i \to -\sigma_i \quad \forall i, \tag{5}$$

Defining the magnetization per spin as:

$$m = \frac{1}{N} \sum_i \sigma_i, \tag{6}$$

This means that for any configuration $\{\sigma\}$ with magnetization m, the flipped configuration $\{-\sigma\}$ has the same energy but magnetization $-m$. As a result, the equilibrium probability distribution satisfies $P(m) = P(-m)$. Although the energies of two configurations with all spin up and spin down are equivalent, thermodynamically they are different. Under such a condition, the system exhibits *spontaneous symmetry breaking*. The phrase refers to the fact that, below a critical temperature T_c, the equilibrium state in the thermodynamic limit does not sample both symmetry

related phases equally. Instead, the system develops two distinct ordered phases characterized by a nonzero magnetization,

$$m \to \pm m_0(T), \qquad (T < T_c), \tag{7}$$

where $m_0(T) > 0$ is the magnitude of the order parameter. Physically, low temperature suppresses domain walls and the typical configurations are dominated by large aligned domains. In the infinite system limit one of the two orientations persists. In the case of two possible states being $\sigma_i = \pm 1$, the magnetization per spin is $m \in [-1, 1]$. In the case $h = 0$ and finite size lattices, it is sensible to take the estimator of order parameter as $\langle |m| \rangle$, where it is in range $[0, 1]$. This is generally used in simulations.

3 Methods

To study equilibrium and domain coarsening, we simulate the 2D ferromagnetic Ising model ($h = 0$) on a $L \times L$ square lattice with total spin number $N = L^2$ using periodic boundary conditions. We set $J = 1$ and $k_B = 1$ for simplicity. For the equilibrium study, which requires longer windows, a Python script was converted into a .C script for faster convergence and run parallel on a High Performance Computing (HPC) cluster. Domain growth and data analysis are implemented in Python.

3.1 Metropolis Monte Carlo

Metropolis Algorithm is employed in this study. Starting from an initial configuration, we evolve the system using single spin Metropolis updates. A trial move flips a randomly chosen spin $\sigma_i \to -\sigma_i$ which produces an energy change ΔE. This move is accepted with probability

$$p = \min\left(1, e^{-\beta \Delta E}\right), \tag{8}$$

and rejected otherwise. One Monte Carlo sweep is defined as N such trial updates.

3.2 Measured observables

For a spin configuration $\{\sigma\}$ on an $L \times L$ lattice ($N = L^2$), the magnetization per spin is measured

$$m = \frac{1}{N} \sum_{i=1}^{N} \sigma_i, \tag{9}$$

and report the estimator -which is the order parameter- $\langle |m| \rangle$ in finite systems with various different lattice sizes. We also measure the energy per spin using the convention that counts each bond once,

$$e \equiv \frac{E}{N} \tag{10}$$

3.3 Equilibration and convergence criterion

A key issue in this model is deciding when the system has equilibrated at a given temperature. In our implementation, equilibration is detected by monitoring the stability of both the absolute magnetization and the energy per spin as functions of Monte Carlo sweep number. After each sweep t we record

$$M_t = |m(t)|, \qquad E_t = e(t). \tag{11}$$

We then calculate window averaged values over two consecutive windows of length w:

$$\overline{M}_{\text{recent}} = \frac{1}{w}\sum_{k=0}^{w-1} M_{t-k}, \qquad \overline{M}_{\text{prev}} = \frac{1}{w}\sum_{k=0}^{w-1} M_{t-w-k}, \tag{12}$$

and similarly $\overline{E}_{\text{recent}}, \overline{E}_{\text{prev}}$ for the energy. We declare equilibration when the relative changes of not only one, but both observables fall below a tolerance `tol`:

$$\delta_M = \frac{\left|\overline{M}_{\text{recent}} - \overline{M}_{\text{prev}}\right|}{\left|\overline{M}_{\text{prev}}\right| + \epsilon}, \qquad \delta_E = \frac{\left|\overline{E}_{\text{recent}} - \overline{E}_{\text{prev}}\right|}{\left|\overline{E}_{\text{prev}}\right| + \epsilon}, \tag{13}$$

and require $\delta_M <$ `tol` and $\delta_E <$ `tol` simultaneously. Here ϵ is a small regularizer to avoid division by zero. We also enforced a minimum burn in time $t_{\text{eq,min}}$ and at least two complete windows before testing convergence. If convergence is not reached by a maximum allowed time $t_{\text{eq,max}}$, the simulation proceeds to the measurement stage anyway, but $t_{\text{eq,max}}$ is chosen large enough that this is rare except near criticality. This condition also lowers the required computational expense to reach equilibrium.

3.4 Practical Methods

Critical slowing down is very impactful on larger system sizes, where the time required to reach equilibrium becomes severe. To compensate this, our implementation rescales the equilibration and measurement sweep counts with system size using an exponent. Taking a reference system size $N_{\text{ref}} = 64$ and an effective exponent $z = 2$, the time scale factor is

$$f(L) = \left(\frac{L}{64}\right)^z. \tag{14}$$

The selection of $N_{\text{ref}} = 64$ as the reference size is simply because it is the minimum lattice size we use in this study. Equilibration and measurement lengths are then scaled as

$$t_{\text{eq,min}} \propto f, \qquad t_{\text{eq,max}} \propto f, \qquad t_{\text{meas}} \propto f, \tag{15}$$

and the convergence window is increased more gently as $w \propto \sqrt{f}$. For each temperature we run statistically independent simulations, each consisting of equilibration until the convergence criterion is satisfied or a maximum time is reached. A measurement stage of length t_{meas} sweeps in which we accumulate $|m|$ and e. For a replica, we report time averages on the measurement window:

$$\langle|m|\rangle_{\text{time}} = \frac{1}{t_{\text{meas}}}\sum_{t=1}^{t_{\text{meas}}} |m(t)|, \qquad \langle e\rangle_{\text{time}} = \frac{1}{t_{\text{meas}}}\sum_{t=1}^{t_{\text{meas}}} e(t). \tag{16}$$

Across replicas, we compute the sample mean and the standard error (SE),

$$\overline{X} = \frac{1}{R}\sum_{r=1}^{R} X_r, \qquad \mathrm{SE}(X) = \frac{s_X}{\sqrt{R}}, \qquad s_X^2 = \frac{1}{R-1}\sum_{r=1}^{R}(X_r - \overline{X})^2, \tag{17}$$

with $R = \texttt{reps}$ and $X \in \{\langle|m|\rangle_{\mathrm{time}}, \langle e\rangle_{\mathrm{time}}\}$. These SE values are what we plot as error bars in the equilibrium results.

3.5 Domain Growth

To study coarsening, we consider transition from a disordered high T state to a target temperature T (around criticality, T_c). Starting from a random initial lattice, we evolved the system under the same Metropolis update and analyzed how a characteristic domain length scale $L(t)$ grows with time (measured in Monte Carlo sweeps, again).

For non conserved order parameter dynamics in the Model A, theory and simulations predict algebraic growth

$$L(t) \sim t^{1/z_d}, \tag{18}$$

with a coarsening exponent $z_d \simeq 2$. But in practice, finite size effects eventually saturate growth when $L(t)$ becomes comparable to L and domain length fluctuates around a constant peak value.

3.5.1 Cluster recognition (Floodfill)

Cluster recognition is our method to recognize domains and calculate $L(t)$. We select sweep times t, and identify connected clusters of like spins. A floodfill algorithm labels each connected component and returns its area A_c. Area is defined as the number of connected and parallel spins in a cluster. From the set of clusters, a linear domain scale can be estimated by converting area to length. Hence, linear size for the cluster can be associated with $A_c^{1/2}$. A simple choice is the area weighted estimator

$$L_{\mathrm{cl}}(t) = \frac{\sum_c A_c(t)\sqrt{A_c(t)}}{\sum_c A_c(t)} \tag{19}$$

$$L_{\mathrm{cl}}(t) = \frac{\sum_c A_c^{3/2}}{\sum_c A_c}, \tag{20}$$

which has the dimensions of length and emphasizes the clusters that dominate. We compute $L_{\mathrm{cl}}(t)$ for 30 independent runs and report the mean and standard error across runs.

3.6 Computational Details

To reduce computational time of the simulations, the temperature and replica pairs (T_i, r) are distributed across MPI worker ranks using a master worker scheduling scheme. The master

maintains a task queue of all (i, r) pairs, sends tasks to workers, and collects results until all tasks complete. Here, an important detail is reproducibility and each replica is seeded deterministically using a base seed `seed` plus integer offsets that depend only on (i, r) (and not on MPI rank). Therefore, changing the number of MPI ranks does not change the numerical outcomes, it changes only the run time.

4 Results and Discussion

4.1 Equilibrium observables and the critical temperature

We first studied equilibrium behavior by measuring our estimator $\langle |m| \rangle$ and the energy per spin e as functions of temperature for several lattice linear sizes L. For each temperature point, we performed $R = 30$ independent replicas and report the replica mean with standard error (SE) error bars for $\langle |m| \rangle$. The simulation parameters for equilibrium runs can be seen in the below

Table 1: Simulation parameters used in the equilibrium runs for estimating $T_c(L)$.

Parameter	Value	Role in the simulation
`reps`	30	Replicas for each measurement point.
`meas_sweeps`	20000	Number of MC sweeps in the measurement stage used to compute the time averaged observables $\langle \lvert m \rvert \rangle_{\text{time}}$ and $\langle e \rangle_{\text{time}}$ after equilibration.
`max_sweeps`	100000	Maximum number of equilibration sweeps allowed before forcing the simulation to proceed to the measurement.
`window`	7000	Window length w (in sweeps) used in the convergence test. The code compares means over two consecutive windows. for both $\lvert m \rvert$ and e.
`tol`	10^{-4}	Relative tolerance for declaring equilibrium $\delta_M <$ `tol` and $\delta_E <$ `tol`.

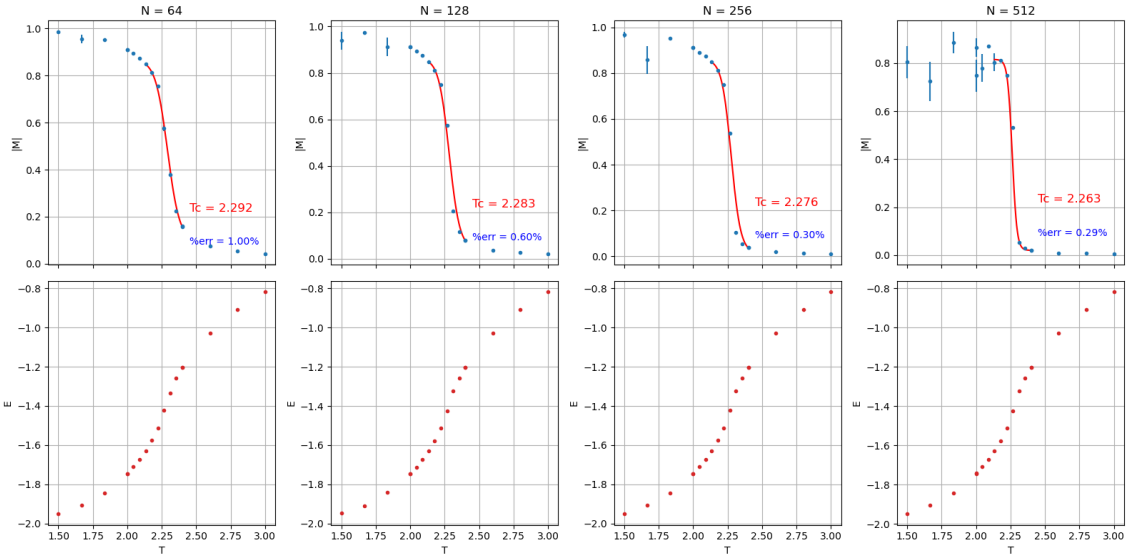

Figure 1: Equilibrium temperature sweep for several lattice sizes, denoted as N. (Top row) Replica averaged $\langle |m| \rangle$ with SE error bars. The red curve is a smooth sigmoid fit used to locate an effective critical temperature $T_c(L)$ (annotated in each panel). (Bottom row) Mean energy per spin $e(T)$, showing a pronounced change in curvature near the same temperature region.

Figure 1 shows the resulting curves for $L = 64, 128, 256, 512$ over the range $T \in [1.5, 3.0]$. $\langle |m| \rangle$ is close to unity at low temperatures (ordered), while it rapidly decreases to values near zero above the transition region (disordered) as expected. Increasing system size makes this drop sharper, which reflects reduced finite size rounding of the phase transition.

For the largest lattice ($L = 512$), the lowest temperature points show noticeably larger scatter/error bars in $\langle |m| \rangle$ compared to smaller sizes. This is consistent with the fact that Metropolis dynamics slows down with system size. Such lattice sizes make equilibration and independent sampling harder unless the measurement window and/or maximum equilibration sweeps are increased tremendously. Despite this, the transition region and the extracted $T_c(L)$ values remain consistent and exhibit the expected finite size trend toward $T_c^{(\infty)}$. Hence, we did not use overly extended periods of time to gather the data.

4.1.1 Estimate of T_c

To obtain a estimate of the critical temperature for each lattice size L, we fitted the measured order-parameter curve $\langle |m| \rangle(T)$ in a restricted temperature window around $T \in (2.1, 2.5]$, where the drop is steepest. The fit was performed using a smooth hyperbolic tangent,

$$f(T) = a + b \tanh\left(\frac{T_c - T}{w}\right), \tag{21}$$

where a and b set the vertical offset and amplitude, $w > 0$ controls the transition width, and the parameter T_c corresponds to the inflection point (midpoint) of the fitted curve. We therefore

identify the fitted value of T_c. The parameters (a, b, T_c, w) were obtained by non linear least squares (`curve_fit`). Initial guesses were chosen from the data. By finding the location of the inflection point of the fit, we were able to find T_c. The extracted critical values are

$$T_c(64) = 2.292, \quad T_c(128) = 2.283, \quad T_c(256) = 2.276, \quad T_c(512) = 2.263. \tag{22}$$

These estimates drift systematically with size toward the exact Onsager critical temperature for the finite 2D Ising model (with our parameters $J = k_B = 1$),

$$T_c^{(\infty)} = \frac{2}{\ln\bigl(1+\sqrt{2}\bigr)} \approx 2.269185. \tag{23}$$

The relative deviation $\%\,\mathrm{err} = |T_c(L) - T_c^{(\infty)}|/T_c^{(\infty)} \times 100$ decreases with increasing L, consistent with finite size scaling expectations (Table 2).

Table 2: Finite size estimates of the critical temperature from the $\langle|m|\rangle$ fits, compared to the exact value of $T_c^{(\infty)} \approx 2.269185$.

L	$T_c(L)$	$\%\,\mathrm{err}$
64	2.292	1.00%
128	2.283	0.60%
256	2.276	0.30%
512	2.263	0.29%

4.1.2 Energy per spin

The energy per spin $e(T)$ increases monotonically with temperature as seen in Fig. 1, bottom row. It approaches the expected low temperature value near $e \approx -2$. It becomes less negative as thermal disorder increases (higher energy phase).

4.2 Domain Growth

We quantified coarsening after a temperature quench by measuring the characteristic domain size $L_{\mathrm{cl}}(t)$ obtained from the Floodfill cluster recognition method. Simulations were performed on a $L = 128$ lattice with 30 independent replicas for each temperature $T \in \{1.90, 2.05, 2.20, 2.35\}$. Figure 2 shows the averaged $L_{\mathrm{cl}}(t)$ with shaded standard error.

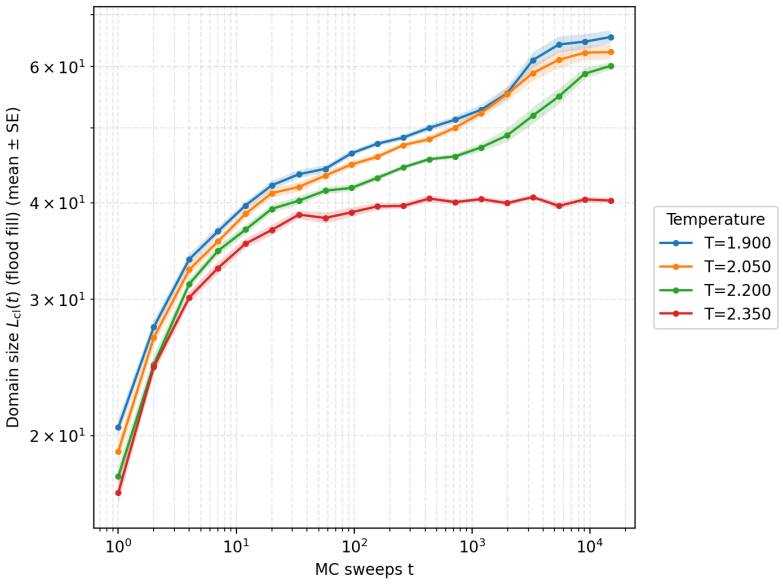

Figure 2: Domain size $L_{\mathrm{cl}}(t)$ from Floodfill cluster recognition (mean ± SE over 30 replicas) for different temperatures with shaded errors.

A rapid early growth is observed for all temperatures and domains form quickly from the initially random configuration. $L_{\mathrm{cl}}(t)$ increases steeply over the first decades in time. At later times the growth becomes slower and temperature dependent. For $T = 1.90$, 2.05, and 2.20 (all below the exact T_c, coarsening continues throughout the measurement window, where lower temperatures producing larger domains at fixed time. In contrast, for $T = 2.35 > T_c$ the curve clearly saturates around $L_{\mathrm{cl}} \approx 40$, consistent with the absence of true phase separation above T_c. There instead of indefinite growth the system approaches a finite correlation length set by thermal variations.

To test for power law growth that we mentioned, we fitted

$$L_{\mathrm{cl}}(t) \sim t^n, \tag{24}$$

in log log scale with the fit performed over the initial scaling window highlighted in Fig. **??**. The fitted exponents n are summarized in Table 3.

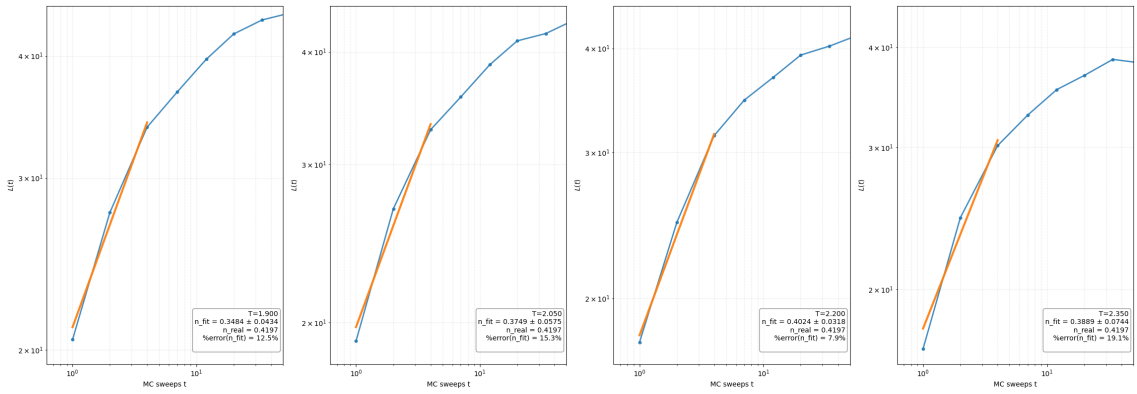

Figure 3: Early time log log growth of $L_{\mathrm{cl}}(t)$ for each temperature. The highlighted segment indicates the fit window used to extract the growth exponent n.

Table 3: Floodfill coarsening exponents extracted from the early time log log fits in Fig. 3.

Temperature	n_{fit}
$T = 1.900$	0.3484
$T = 2.050$	0.3749)
$T = 2.200$	0.4024
$T = 2.350$	0.3889

Across the studied temperatures the exponent lies in the range $n \simeq 0.35$-0.40. The extracted value is slightly temperature dependent, but within uncertainties the results are broadly consistent with early coarsening regime. We emphasize that these fits are performed at early times since at later times the growth bends due to finite size effects.

5 Conclusion

In conclusion, our equilibrium run allowed us to calculate a data driven T_c, which is very close to the Onsager critical temperature, with maximum error percentage of 1 for a very finite lattice of $L = 64$, our minimum lattice size. Larger lattice sizes showed less error as expected. For the domain coarsening, we studied several temporatures around criticality and quantified the growth rate. Our results show that, in the chosen window, the acquired grow exponent is close to the theoretical value, with some acceptable errors. The temperature dependence in the coarsening curves was also clearly observed. Lower temperature values produce larger domains, while higher temperatures produce smaller.

Overall, our results demonstrate that Monte Carlo simulations of the 2D Ising model can reliably capture both the equilibrium phase transition and the domain growth. The equilibrium observables reproduce a critical temperature consistent with Onsager's exact value even with finite size problems. And below criticality, the system shows domain growth with near theoretical power law exponent.